JOURNAL OF THERMOPHYSICS AND HEAT TRANSFER
Vol. 12, No. 3, July–September 1998

# Test Results of Water and Methanol High-Speed Rotating Heat Pipes

R. Ponnappan* and Q. He†
*UES, Inc., Dayton, Ohio 45432*
and
J. E. Leland‡
*U.S. Air Force Research Laboratory, Wright–Patterson Air Force Base, Ohio 45433*

**The existing rotating heat pipe (RHP) technology was examined and further developed for possible cooling applications in high-speed rotating electrical machines required for future designs of more-electric aircraft. Several technical papers covering the results of the design, fabrication, and testing of the RHP hardware in the low-to-intermediate rotational speeds from 500 to 7500 rpm have been published in recent years. In this investigation, performance results are presented for stainless steel 316—methanol and stainless-steel 316—water high-speed rotating heat pipes (HSRHPs) that were tested at speeds up to 30,000 rpm for the first time in the history of RHP research. The HSRHPs were cooled by air and oil jets in separate tests to compare their relative performances. Interesting temperature profiles and test results are presented for the HSRHPs that were heated by an induction heater and tested in the temperature range of 20–250°C for power inputs from 250 to 1300 W.**

## Nomenclature

| | | |
|---|---|---|
| $A_c$ | = | condenser area, $cm^2$ |
| $a$ | = | centrifugal acceleration, $m/s^2$ |
| $D$ | = | outer diameter of the RHP, cm |
| $h_c$ | = | heat transfer coefficient, $W/m^2$ K |
| $G$ | = | ratio of induced acceleration to gravitational acceleration ($a/g$), nondimensional |
| $g$ | = | acceleration from gravity, $m/s^2$ |
| $L_c$ | = | condenser length, m |
| $N$ | = | rotational speed, rpm |
| $Q$ | = | heat transport, W |
| $Q_{cal}$ | = | heat removed by oil or air, W |
| $Q_{in}$ | = | heat input to the HSRHP, W |
| $Q_{loss}$ | = | heat loss to the ambient, W |
| $Q_{ms}$ | = | heat generated by magnetic seals, W |
| $Q_{tran}$ | = | heat transported from evaporator to condenser, W |
| $R$ | = | inner radius of RHP, cm |
| $T_{av}$ | = | average temperature, °C |
| $T_e$, $T_a$, $T_c$ | = | evaporator, adiabatic, condenser temperature, °C |
| $T_s$, $T_v$ | = | saturation, vapor core temperature, °C |
| $\Delta T$ | = | temperature difference, °C |
| $\Delta T_{fc}$ | = | temperature difference across the condensate film in condenser, °C |
| $\omega$ | = | angular velocity, rad/s |

## Introduction

DESIGNERS are beginning to realize the severity of the thermal problems in advanced rotating electrical machines. Efficient, lightweight, and fault-tolerant high-speed electrical machines such as alternators, generators, actuator-motors, integral starter/generators, etc., are required for advanced military and commercial aircraft and machine tool applications. These machines are built using state-of-the-art technologies that focus on shrinking the size and increasing the power-to-weight ratio. Of particular interest here are the permanent magnet and the switched reluctance types of rotor technologies that are improvements over traditional wound-rotor technology of the past. Because of the dual-use (commercial as well as military) potential of these machines, the government agencies are promoting increased attention in perfecting these technologies through their more-electric aircraft (MEA) initiatives.[1–3] Thermal management of the rotors in these machines has been a challenging problem for the heat transfer experts. There are a variety of parameters such as high speed, windage loss, high acceleration loadings, difficulty in measuring temperature in rotation, lack of a proper thermal coupling between the rotor and stator, etc., which influence the thermal characteristics of the rotor in an electrical machine. For example, power densities of 4.4–11.0 kW/kg and rotor tip velocities up to 313.9 m/s are not uncommon, and nearly 20% of the rated power capacity is dissipated as waste heat within the machine.

In the present research, a rotating heat pipe (RHP) design problem was conceived based on the requirement of cooling a developmental switched reluctance machine (SRM) type integrated power unit (IPU) whose rotor generates about 2000 W as core losses. The rotor's safe operating temperature is to be kept below 388°C. The rotor can operate at 40,000 rpm and has a 2.54-cm o.d. and a 12.3-cm long shaft that houses the RHP.

### Background History

A vast majority of studies found in the literature have been performed for speeds of less than 3000 rpm.[4] One of the significant contributors to the RHP literature experimentally and analytically studied a tapered rotating noncapillary-driven heat pipe.[5] A stainless-steel pipe was fabricated for testing and results were presented for water, ethyl alcohol, and Freon-113. The analytical results were obtained by an extended version of the Nusselt film condensation method. Experimental results were obtained for rotational speeds of 700 and 2800 rpm. The agreement between the experimental and analytical results were within ±20%.

Received July 14, 1997; revision received Feb. 17, 1998; accepted for publication Feb. 23, 1998. 

*Principal Research Scientist. Senior Member AIAA.
†Research Scientist; currently Mechanical Engineer, Yellow Springs Instruments, Inc., Yellow Springs, OH. Member AIAA.
‡Research Engineer, Power Division (AFRL/PRPG). Member AIAA.

Daniels and Al-Jumaily[6] experimentally studied a rotating tapered heat pipe at speeds of 600, 800, 1000, and 1200 rpm. An analytical model was presented in which expressions for the film thickness distribution, film velocity, and local heat flux along the condenser were developed. The heat pipe was fabricated out of solid copper and three different working fluids were examined: Arcton 113, Arcton 21, and water. The experimental and analytical results were in good agreement for Arcton 113 and Arcton 21. However, there was no agreement for water.

Vasiliev and Krolenek[7] analytically and experimentally studied the use of longitudinal grooves in the condenser as a mechanism to enhance heat transfer. Results were presented for 1000–2000 rpm and the agreement between the experimental and analytical results was good. Peterson and Wu[8] reviewed RHP literature published from 1964 to 1990 and compiled interesting results from authors of three different experimental studies on horizontal RHPs without internal taper. They noted that the evaporation and condensation heat transfer coefficients varied with $G$ in a hysteresis fashion for the on-axis rotation acceleration ranging from $G = 0$ to 65.7. The destruction and critical acceleration levels referring to the collapse and formation of liquid annulus occurred at $G = 10$ and 20, respectively.

Harley and Faghri[9] numerically solved the Navier–Stokes equations for a rotating tapered heat pipe that was modeled after the hardware tested by Daniels and Al-Jumaily. But Harley and Faghri could not compare and validate their results with the experimental results obtained by Daniels and Al-Jumaily because of the latter's assumption of the outer wall heat transfer coefficient. It may be noted that the $G$ levels reported in all the previously mentioned studies are two orders of magnitude smaller than the levels studied in the present work.

Initially, a low-speed, stainless-steel-water version of an RHP that was 2.54-cm o.d., and 45.6-cm long, was designed, fabricated, and tested up to 3500 rpm. A radiatively coupled nichrome heater and air–water mist cooling arrangement together with infrared temperature measurement were employed in testing this RHP up to 225°C and 1500 W.[10] The thermal management issues and problems relating to the advanced electrical machines were identified and compiled including a literature search on this topic.[4,11] Additional tests and improvements were made to boost the speed to 7000 rpm and the power to 2250 W using a better mechanical support system and induction heating, respectively.[12] A high-speed RHP design involving a shorter length (30 cm nominal) and ceramic ball-bearing supports with critical speeds higher than 40,000 rpm was undertaken. The dynamic balancing and dynamic shaft seal problems were overcome with the successful spinning of this high-speed rotating heat pipe (HSRHP) up to 32,000 rpm in a test rig developed for this purpose.[11,13] The low-speed RHP was reprocessed and filled with methanol working fluid and tested to compare the results with the water-filled RHP. Significant differences in heat transport capacities, 2250 W for the water-RHP vs 1200 W for the methanol-RHP, and symptoms of noncondensible gas generation in the water-RHP were observed. The water-RHP showed a large $\Delta T$ of ~80°C across the evaporator and condenser, whereas the methanol-RHP performed in near-isothermal conditions.[14]

### Scope

The scope of the present study was to extend the design, fabrication, and performance evaluation of the RHP into the more difficult speed regime of 5000–30,000 rpm in the horizontal on-axis mode of testing and using air and oil cooling arrangements that are preferred over the air–water mist cooling for aircraft applications. The goal was to demonstrate the successful functioning of the various elements such as spray-nozzles, magnetic seals, calorimetric measurements, and dynamics at high speeds. Also, it was the aim of this study to evaluate the performance characteristics of the two different working fluids, water and methanol, in the container metal, stainless-steel 316, with respect to noncondensible gas generation, heat transport capacity, and axial temperature profile and corroborate with the theoretical predictions made based on the Nusselt condensation model of Daniels and Al-Jumaily.[6]

## Experimental Work

### Test Hardware

Two identical sets of HSRHP hardware shown in Fig. 1a were fabricated, one for water and the other for methanol filling. The physical details are listed in Table 1. The dimensional parameters are as follows: material = stainless-steel 316, length of overall/bearing centers = 37.2/26.67 cm, active length (vapor space) = 22.89 cm, o.d. = 2.54 cm, condenser i.d. = 1.46/1.91 cm, evaporator i.d. = 1.91 cm, internal surface area = 132.63 $cm^2$, internal volume = 57.44 $cm^3$, effective lengths (evaporator/adiabatic/condenser) = 7.6/2.8/8.9 cm, adiabatic length at each end = 2.8 cm, condenser taper (half-cone) = 1.0 deg, evaporator internal surface = v-threads, 40/cm, and external surface finish = black paint; $\varepsilon = 0.9$. Each set of HSRHP was made of a main tubular body, two end caps and, a fill tube that were joined by electron beam welding. The design of the main tube with open ends facilitated easy machining of the internal taper and v-threads. Before welding the end caps to the tube, the machined parts were thoroughly cleaned as per heat-pipe cleaning and conditioning procedures that included placement of the main tube in an electric furnace and heating in air at 400°C for 1 h, which supposedly inhibited noncondensible gas generation.[15] A final finish-machining and dynamic balancing operation preceded the filling and sealing processes. The HSRHP test hardware were individually vacuum baked at $3 \times 10^{-7}$ torr and 340°C for over 72 h and then filled with the appropriate fluid by the vacuum suction transfer method. The fill tube was crimped in situ and sealed by welding. A photographic view of one of the HSRHPs is shown in Fig. 1b. A complete description of the design and fabrication can be seen in Ref. 11.

### Test Setup

The experimental test setup consisted of the following subsystems: 1) ball-bearing support system with precision align-

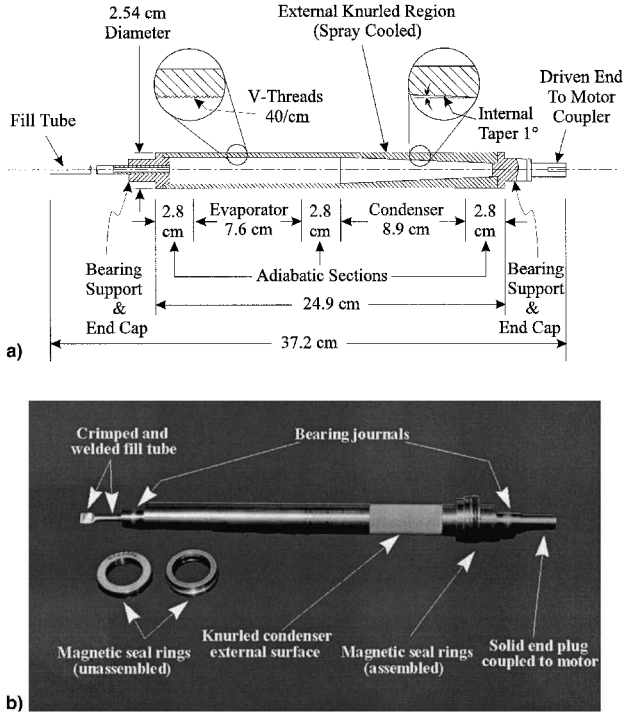


**Fig. 1 a) Overall details and b) photographic view of the HSRHP.**

**Table 1 HSRHP test parameters**

| | Water RHP | Methanol RHP |
|---|---|---|
| Working fluid (type/quality) | Water (degassed deionized; resistance = 18 MΩ-cm) | Methanol (analytical grade; 99.99% pure) |
| Quantity filled | 0.0105 kg | 0.0057 kg |
| Weight of filled RHP | 0.627 kg | 0.620 kg |
| Liquid fill-to-internal volume ratio at 25°C | 18.3% | 12.6% |
| Temperature range | 20–250°C | 20–150°C |
| Design heat transport capacity: (refer to Figs. 6 and 7) | 2000 W (at 30,000 rpm; $T_{av}$ = 140°C; $\Delta T_{fc}$ = 10°C) | 1000 W (at 30,000 rpm; $T_{av}$ = 140°C; $\Delta T_{fc}$ = 20°C) |

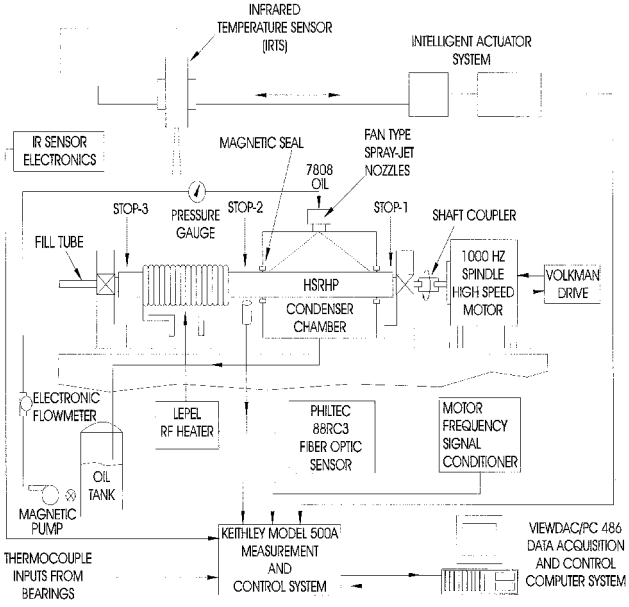


**Fig. 2 Schematic diagram of the HSRHP test setup.**

ment; 2) high-speed drive spindle and speed control with dynamic braking; 3) noncontact induction heating coil for supplying calibrated heat input to the RHP; 4) spray-cooling chamber with magnetically attached rotary seals for the condenser cooling and calorimetry; 5) noncontact infrared temperature measuring system with programmable actuator and control; 6) shaft vibration and displacement monitoring sensors with safety interlocks; and 7) Keithley's Viewdac data acquisition and control system interfaced with a Keithley model 500A measurement unit.

Figure 2 shows a schematic diagram of the setup. The HSRHP could be spun about its longitudinal axis at any speed from 5000 to 30,000 rpm, which is below the estimated first critical speed of 37,500 rpm. The angular-contact ball bearings were able to be preloaded with a predetermined axial thrust to keep the radial stiffness of the bearings above 17,512.8 kN/m. Oil-jet and air-jet cooling of the RHP condenser were possible with the same fan-type nozzles, except that the condenser chamber was not necessary for the air-jet cooling mode. Two unavoidable drawbacks were present in the oil-jet cooling arrangement. These were the parasitic heat addition by the magnetic seals and the inability to measure the condenser temperatures using the infrared (IR) temperature sensor.

### Measurement Uncertainty

The estimated systematic uncertainties of the radio frequency (RF) power input measurement varied from 24.1 to 5.4% for the power level variation from 500 to 2500 W, respectively. The uncertainties for the oil-jet cooled condenser calorimetry output between 250 and 2000 W varied from 12 to 6.1%, respectively. The temperature measurement accuracies were within ±0.5°C for the IR sensors and ±0.3°C for the thermocouples.

### Test Procedure

All of the performance tests on both water and methanol HSRHPs were conducted in horizontal orientation and on-axis rotation mode under steady-state conditions of the test parameters. Typically, the tests were started by flowing the cooling medium, air or oil, first and then spinning the pipe at 5000 rpm followed by the application of the heat input to the evaporator. After allowing the system to attain steady state, which usually took about 30 min, the temperature, flow rate, and power input were recorded. The speed was increased in steps of 5000 rpm until the maximum of 30,000 rpm for the chosen power input and steady-state data were recorded. The condenser cooling rate was varied as desired by adjusting the oil or air flow rate. The spread of the present test parameters were as follows:

1) Power input: 250, 500, 750 W (air-cooled mode); and 250, 500, 750, 1000, 1250, and 1300 W (oil-cooled mode).

2) Speed: 5000–30,000 rpm in steps of 5000 rpm.

3) Flow rate: 14.87 standard $m^3$/h air at 25°C; and 0.87, 1.89, 2.84, and 3.26 lpm oil.

4) Oil temperature: 30–60°C.

5) Jet cooling nozzle arrangement: three nozzles mode (air and oil); and one nozzle mode (oil only).

A total of 35 different test runs covering the preceding settings were performed on the HSRHPs. The cumulative hours of test logged were 34.5 for the methanol pipe and 56 for the water pipe. Axial preloading applied on the bearings was 5.17 N. The vibration levels at the bearing supports measured as velocity varied from 0.0254 to 0.3048 cm/s and the displacement at the midpoint of the pipe remained within ±0.0254 cm.

## Results and Discussion

### Calorimetry

A schematic diagram of the heat balance model for the HSRHP is shown in Fig. 3. Calorimetric measurement was possible with the oil-jet cooling over the condenser length. Under steady-state conditions, the heat balance can be written as

$$Q_{in} - Q_{loss} + Q_{ms} - Q_{cal} = 0 \quad (1)$$

$$Q_{tran} = Q_{in} - Q_{loss} \quad (2)$$

Combining Eqs. (1) and (2), experimental $Q_{tran}$ can be obtained as

$$Q_{tran} = Q_{cal} - Q_{ms} \quad (3)$$

The experimental data output from Viewdac for both HSRHPs were processed to obtain the various terms in the heat-balance equations. Figures 4 and 5 show these details for water and methanol HSRHPs, respectively. The data variation in the $y$ axis for any given heat input reflects the variation in operating speed in the range of 5000 and 30,000 rpm. It can be observed from these figures that roughly 70–80% of the $Q_{in}$ is transported by the HSRHPs.

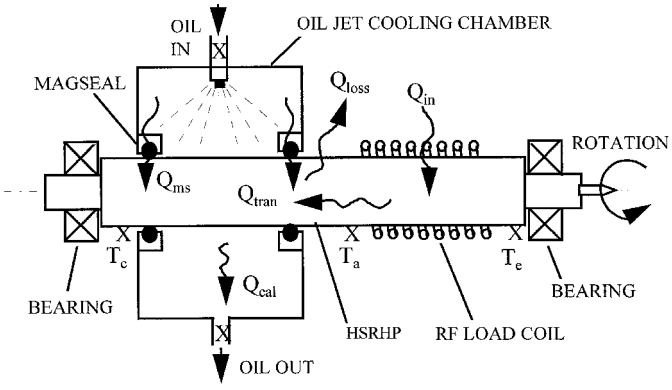


**Fig. 3 Heat balance model.**

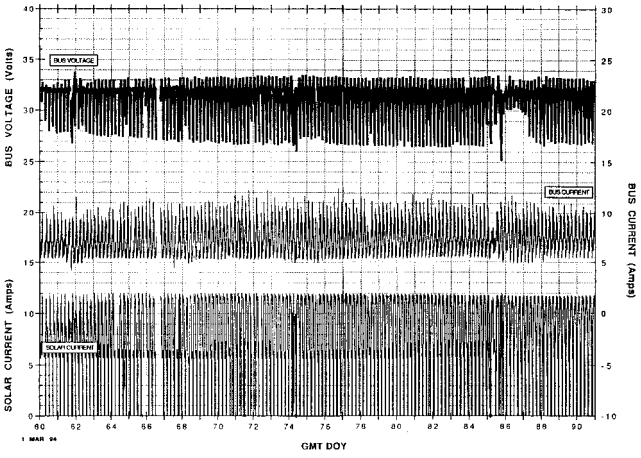


**Fig. 4 Steady-state heat balance data, water HSRHP.**

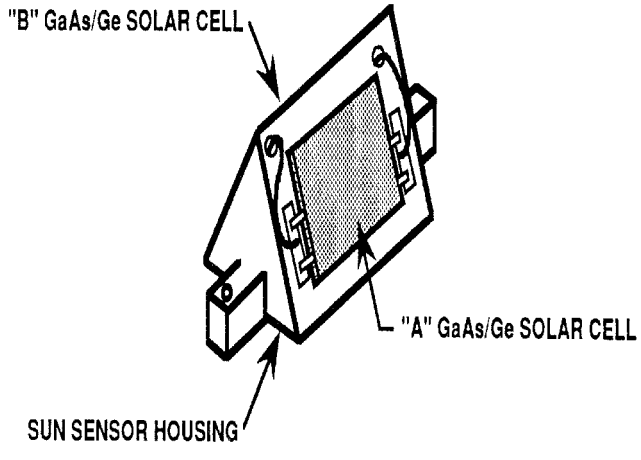


**Fig. 5 Steady-state heat balance data, methanol HSRHP.**

### Heat Transport and Comparison with Theory

The heat transport capacity of a conventional RHP is shown in Ref. 6 to be a function of a group of thermophysical properties of the working fluid and some mechanical parameters associated with the design and on-axis rotation. The group of fluid properties is called the liquid transport factor comprising the density, latent heat, conductivity, and dynamic viscosity. The transport capacity is also a strong function of speed, temperature difference across the condenser liquid film, taper angle, length, and radius of the condenser.

The theoretical and experimental transport capacities of the water and methanol HSRHPs are plotted in Figs. 6 and 7, respectively. The theoretical estimates correspond to an average operating temperature of 140°C, whereas those of the experimental data correspond to a range of operating temperatures that were the result of the actual test conditions imposed on the test. As the vapor-core temperature and $\Delta T_{fc}$ could not be measured, the following approximations were used in deducing the experimental data assuming near-saturation condition of operation and constant wall thickness:

$$T_{av} = 1/3(T_e + T_a + T_c) \tag{4}$$

$$T_v = T_s = 1/2(T_e + T_c) \tag{5}$$

$$\Delta T_{fc} = 1/2(T_e + T_c) - T_a \tag{6}$$

where $T_e$, $T_a$, and $T_c$ are measured data. It may be noted that there was no noncondensible gas blockage in the condenser during the present experiments to seriously affect this approximation. And also, the wall-temperature differences at these measurement spots were assumed to be very small because of the near-adiabatic conditions. This assumption was justified because the calculated convection and radiation heat losses from each of the RHP sections exposed to the ambient showed only less than 11% of $Q_{in}$.

The agreement between the theory of Ref. 6 and the present results is poor for both HSRHPs. The deviation is greater in the case of water HSRHP. There are two reasons attributable to this discrepancy. One is experimental limitation caused by the poor external condenser cooling arrangement of the oil cooling that does not match with the design heat transport of the HSRHPs. Air–water mist cooling might have provided better cooling but it was not used because of mission restrictions

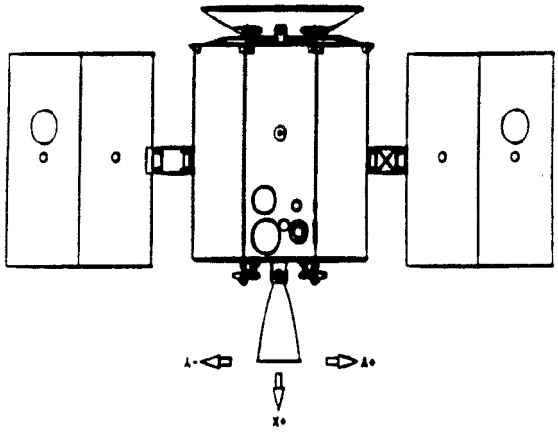

**Fig. 6 Heat transport capacity, water HSRHP.**

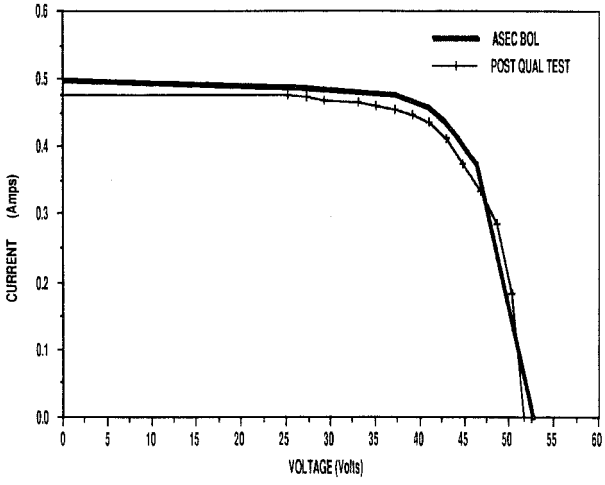


**Fig. 7 Heat transport capacity, methanol HSRHP.**

for aircraft applications. The second reason is the questionable applicability of the Nusselt-type condensation theory of Ref. 6 for the high-speed regime of the present experiment. It may be noted here that centrifugal acceleration levels from $G$ = 1000 to 9000, where $G = a/g = \omega^2 R/g$ and $\omega = 2\pi N/60$, are induced at the inner walls of the HSRHPs with 1.905 cm i.d. for speeds from 10,000 to 30,000 rpm. The effects of the high values of $G$ on the hydrodynamics and condensation/evaporation heat transfer of the liquid film inside these HSRHPs are completely unknown in the context of the RHP research and forms an exploratory area. It appears that the favorable feature of the high speed on the condensate pumping action has the detrimental effect of reducing the evaporative and condensation heat transfer at high values of $G$. A more rigorous theory from a fundamental approach is needed.

The highest heat transport capacity demonstrated in the present tests for the water HSRHP was 1033 W at $T_{av}$ = 197°C and $\Delta T_{fc}$ = 62.5°C and for the methanol HSRHP was 644 W at $T_{av}$ = 170°C and $\Delta T_{fc}$ = 39.6°C. This shortfall in performance compared to the design values in Table 1 is attributed to the poor efficiency of the present external condenser cooling.

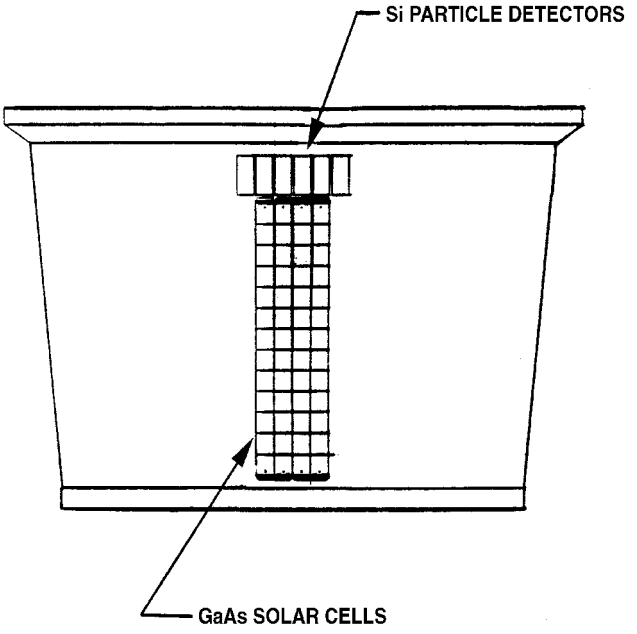


**Fig. 8 Steady-state temperature, $Q_{in}$ = 750 W; air cooling; water HSRHP.**

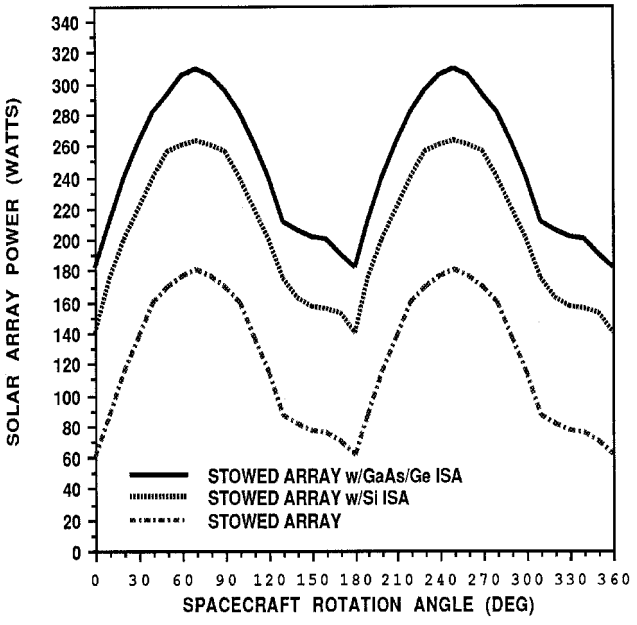


**Fig. 9 Steady-state temperature, $Q_{in}$ = 750 W; air cooling; methanol HSRHP.**

### Axial Temperature Profile

*Air Cooling Mode*

External surface temperatures of the HSRHPs measured at seven spots along the length of the pipes when subjected to a heat load of 750 W and rotation are plotted in Figs. 8 and 9. It may be observed that the temperatures decreased as the speed increased in both heat pipes, which is the expected trend. The air cooling was applied over the condenser through three air nozzles kept 120-deg apart around the pipe and the total airflow rate was 14.87 standard $m^3/h$. The temperature gradients from the midsection to the evaporator and condenser ends signify the gradual change of condensate film thickness occurring inside the pipe. The lowest temperature location is at the middle where the high film thickness is expected. The evaporator to condenser $\Delta T$ variation ranges from 15 to 26°C.

*Oil Cooling Mode*

Figures 10 and 11 show the axial temperature profiles of the HSRHPs measured at three spots for the condenser cooling with the MIL-STD-7808 oil using the fan-type jets kept 120-deg apart and heating the evaporator with 750 W. The trend of temperature gradients from the midsection to the ends is similar to the one observed in the air-cooling mode. However, there is an unexpected behavior of increasing temperature with increasing speed. This anomaly can be attributed to two reasons. One is that the inlet temperature of the oil to the condenser was not constant and the other is the poor contact of the coolant oil with the HSRHP condenser at higher speeds. The latter reason is conceivable as the velocity of the impinging oil-jet is not high enough to overcome the increasing peripheral velocity of the HSRHP with increasing rotational speed. The evaporator to condenser $\Delta T$ variation ranges from 5 to 19°C.

*Effect of Single-Jet Oil-Cooling*

In the interest of improving the transport capacity of the HSRHP, several operational parameters such as increased coolant flow rate, lower coolant inlet temperature, coolant jet ve-

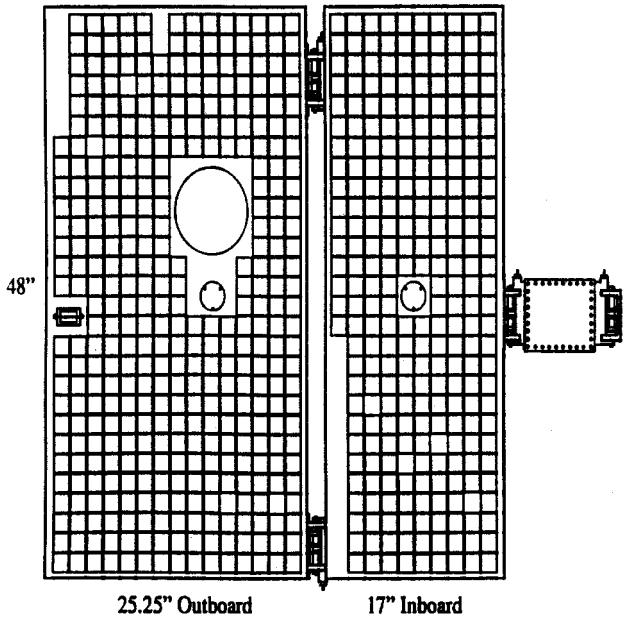


**Fig. 10 Steady-state temperature, $Q_{in}$ = 750 W; oil cooling; water HSRHP.**

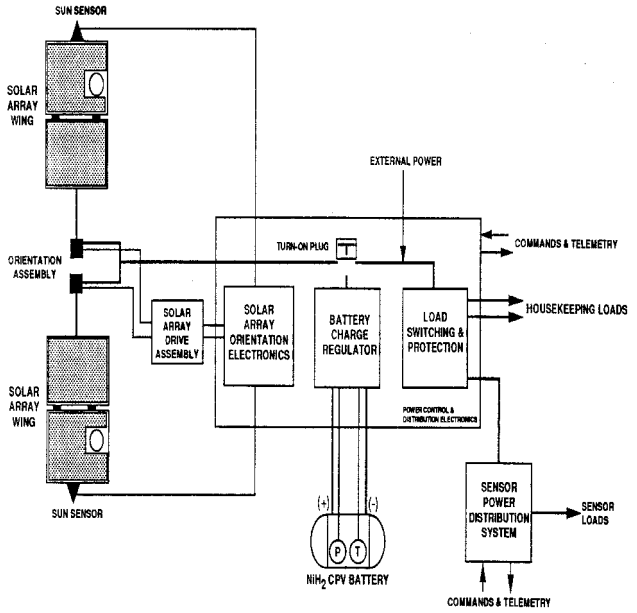


**Fig. 11 Steady-state temperature, $Q_{in}$ = 750 W; oil cooling; methanol HSRHP.**

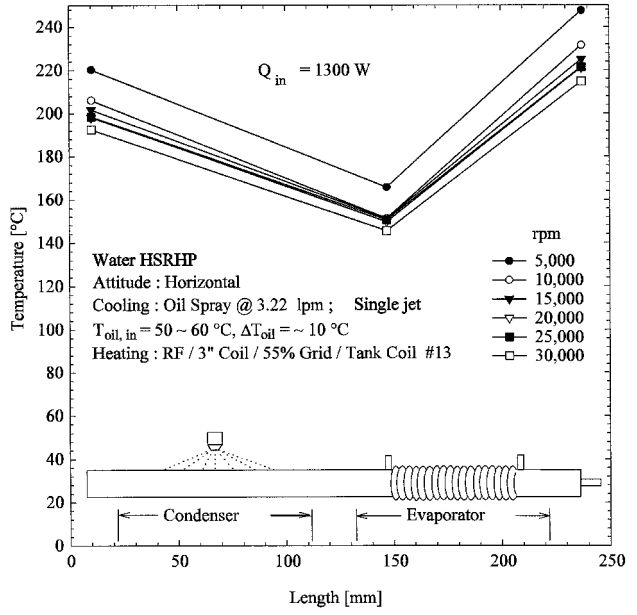


**Fig. 12 Steady-state temperature, $Q_{in}$ = 1300 W; water HSRHP; single-jet-oil cooling.**

locity, etc., were explored. By using only one of the three jets with full flow of oil (3.22 lpm that the pump could deliver), the water HSRHP could be operated up to an input power of 1300 W. A surprising development observed in this test was the expected trend of performance, namely, decreasing temperature with increasing speed. Figure 12 shows the details of this test. Similar results were obtained at a lower heat input. It is clear from this result that the impinging oil-jet velocity is a critical factor in enhancing the external cooling of the condenser.

*Effect of Coolant Flow Rate*

The cooling oil-flow rates were varied from 0.87 to 3.22 lpm for a given heat input and several speeds. It was observed that the temperatures decreased with increase in flow rates for both single and three jet cases.

**Condensate Film $\Delta T$**

The variations of $\Delta T_{fc}$, calculated using Eq. (6), for all of the experimental data available for water HSRHP are plotted as a function of $T_{av}$ as shown in Fig. 13 for air cooling and in Fig. 14 for oil cooling. It is interesting to note that the $\Delta T_{fc}$ increases with increasing speed and decreasing $T_{av}$ for $Q_{in}$ up to 500 W in the air-cooling mode. In contrast $\Delta T_{fc}$ decreases with increasing speed and decreasing $T_{av}$ for $Q_{in}$ = 750 W. In the case of oil cooling, two distinctly different trends are seen for the single- and three-jet cases, as is evident from Fig. 14. The overall trend of increasing $T_{av}$ with increasing $Q_{in}$ is also clear from these graphs.

**Condenser $h_c$**

An average convective heat transfer coefficient for the external cooling of the condenser was calculated for all of the test data available for the water HSRHP using the equation

$$Q_{cal} = h_c A_c (T_{c,av} - T_f) \tag{7}$$

where $T_{c,av} = (T_a + T_c)/2$ for oil cooling or $(T_{c1} + T_{c2} \ldots T_{c5})/5$ for air cooling, $T_f$ = oil inlet or ambient air temperature, and $A_c = \pi D L_c = 71$ cm$^2$. For air cooling, $Q_{cal}$ is assumed to be equal to 0.77 $Q_{in}$. The $h_c$ values for various test situations are plotted in Fig. 15. As noted earlier, the single oil-jet cooling provided the highest $h_c$ compared to the three-jet mode or the air cooling. The highest $h_c$ obtained in these tests is 1230 W/m$^2$ K compared to the range of literature values, 60–1800 W/m$^2$ K, given for convective oil cooling.

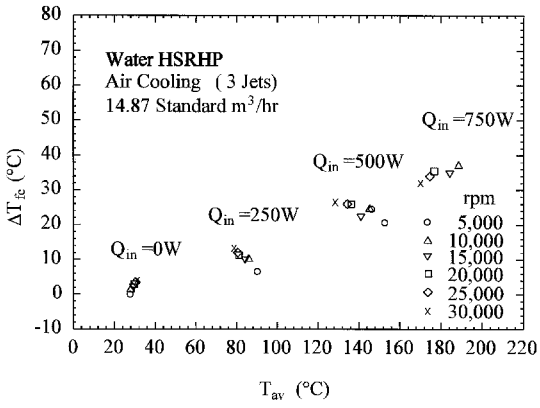


**Fig. 13 Condensate film $\Delta T$ vs average operating temperature, air cooling.**

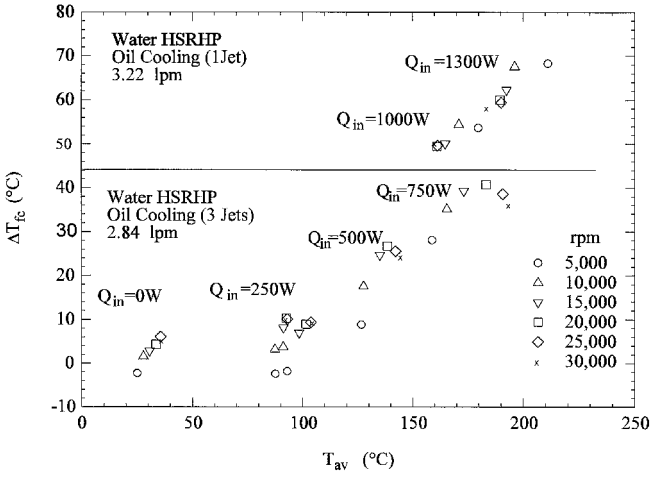


**Fig. 14 Condensate film $\Delta T$ vs average operating temperature, oil cooling.**

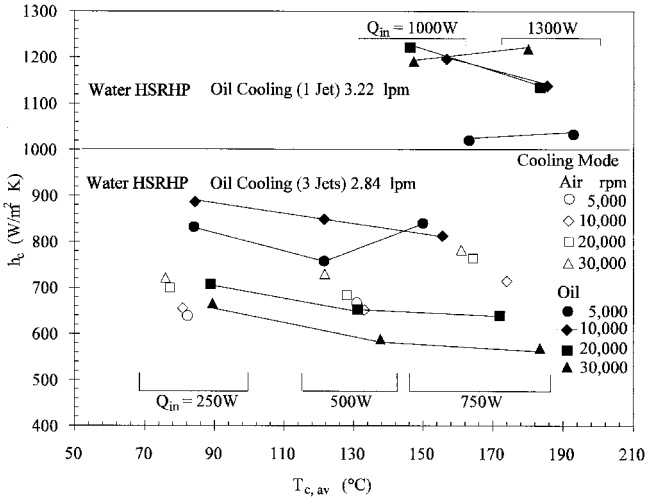


**Fig. 15 External condenser heat transfer coefficient.**

### Material Compatibility

It is generally known in the heat pipe industry that stainless-steel-water, to a large extent, and stainless-steel-methanol, to a small extent, are incompatible envelope-fluid combinations. Experimental results demonstrating this fact have been previously published by the authors.[11,14] Chemical passivation and copper deposition or copper sleeving of the wetted surfaces are methods that could be employed to minimize or eliminate the noncondensible gas-generation problem for producing heat pipes with a long service life in the commercial arena. However, these expensive procedures were believed unnecessary for the present experimental hardware because the high-speed performance could be accomplished with in a short duration of less than 100 h of testing.

## Conclusions

The following are the summary and conclusions of the present research:

1) Two high-speed rotating heat pipes made of stainless-steel 316 and filled with water and methanol working fluids have been designed, fabricated, and tested.

2) These HSRHPs with potential future application in cooling of high-speed rotating electrical machines were tested successfully up to 30,000 rpm for the first time.

3) The single-jet, oil-cooling mode produced the best results in terms of the heat transport capacity, heat transfer coefficient, and temperature difference across the condensate film because of the high velocity of the impinging oil jet.

4) The highest performance numbers demonstrated in the present tests are water HSRHP: $Q_{tran}$ = 1033 W at $T_{av}$ = 197°C and $\Delta T_{fc}$ = 62.5°C and methanol HSRHP: $Q_{tran}$ = 644 W at $T_{av}$ = 170°C and $\Delta T_{fc}$ = 39.6°C.

5) The agreement between the existing Nusselt-type condensation model-based theory and the experimental results is poor. A few plausible reasons for this discrepancy are explained. A new model for heat transfer in high $G$ is necessary.

6) The air cooling offers a simple but limited-capacity HSRHP condenser-cooling alternative to the troublesome oil cooling and potential dynamic oil-seal problems.

7) Both working fluids, water and methanol, are beneficial to the RHP application. The stainless-steel 316-water and stainless-steel 316-methanol envelope material—working fluid combinations worked well in the present study. However, further studies and life tests are suggested to assess the effects of noncondensible gas generation on the useful life of a rotating heat pipe.

## Acknowledgments

This work was funded by the Aero Propulsion and Power Directorate of the Air Force Research Laboratory (AFRL) through Contract F33615-96-C-2680 and supported by the Mechanical Branch's Thermal Laboratory. Technical assistance was provided by J. Tennant (UES, Inc.), R. Carr (UES, Inc.), and D. Reinmuller (AFRL), and publication assistance was provided by D. D. Donley (UES, Inc.). The authors also acknowledge the services of K. Klasing (UES, Inc.) in preparing the final manuscript.

## References

[1]Quigley, R. E., Jr., "More Electric Aircraft," *Proceedings of the IEEE APEC-93 8th Annual Applied Power Electronic Conference and Exposition—APEC '93* (San Diego, CA), Inst. of Electrical and Electronics Engineers, Piscataway, NJ, 1993, pp. 906–911.

[2]Cronin, M. J., "Advanced Power Generation Systems for More Electric Aircraft," Society of Automotive Engineers, TP 912186, Sept. 1991.

[3]Colegrove, P. G., "Integrated Power Unit for a More Electric Airplane," AIAA Paper 93-1188, Feb. 1993.

[4]Ponnappan, R., Leland, J. E., and Beam, J. E., "Thermal Management Issues of Rotors in Rotating Electrical Machines," Society of Automotive Engineers, Paper 942184, Oct. 1994.

[5]Marto, P. J., "An Analytical and Experimental Investigation of Rotating Non-Capillary Heat Pipes," NASA CR-130373, Sept. 1973.

[6]Daniels, T. C., and Al-Jumaily, F. K., "Investigations of the Factors Affecting the Performance of a Rotating Heat Pipe," *International Journal of Heat and Mass Transfer*, Vol. 18, No. 7/8, 1975, pp. 961–973.

[7]Vasiliev, L. L., and Khrolenok, V. V., "Study of a Heat Transfer Process in the Condensation Zone of Rotating Heat Pipes," *Heat Recovery Systems*, Vol. 3, No. 4, 1983, pp. 281–290.

[8]Peterson, G. P., and Wu, D., "A Review of Rotating and Revolving Heat Pipes," American Society of Mechanical Engineer, Paper 91-HT-24, July 1991.

[9]Harley, C., and Faghri, A., "Two-Dimensional Rotating Heat Pipe Analysis," *Journal of Heat Transfer*, Vol. 117, No. 1, 1995, pp. 202–208; also *Heat Pipe Science and Technology*, Taylor and Francis, Washington, DC, 1995, p. 471.

[10]Ponnappan, R., Leland, J. E., and Beam, J. E., "Rotating Heat Pipe for Cooling of Rotors in Advanced Generators," AIAA Paper 94-2033, June 1994.

[11]Ponnappan, R., "Thermal Management Research Studies Volume 2—Rotating Heat Pipe," U.S. Air Force Research Lab., Final Rept. WL-TR-97-2002, Wright–Patterson AFB, OH, Sept. 1996.

[12]Ponnappan, R., and Leland, J. E., "High Speed Rotating Heat Pipe for Aircraft Applications," Society of Automotive Engineers, Paper 951437, May 1995.

[13]Streby, M. A., Ponnappan, R., Leland, J. E., and Beam, J. E., "Design and Testing of a High Speed Rotating Heat Pipe," Intersociety Energy Conversion Engineering Conf., Paper 96301, Aug. 1996.

[14]Ponnappan, R., Leland, J. E., and Beam, J. E., "Comparison of Performance Results for Water and Methanol Rotating Heat Pipes," AIAA Paper 96-0477, Jan. 1996.

[15]Dunn, P. D., and Reay, D. A., *Heat Pipes*, 2nd ed., Pergamon, New York, 1978, p. 163.